

## Molecular docking, synthesis, and cytotoxic evaluation of novel quinazoline-quinazolinone hybrid compounds

Majid Azarmi<sup>1</sup>, Saman Rahimi<sup>1</sup>, Maryam Hormozi<sup>2</sup>, and Rezvan Rezaeinasab<sup>1,\*</sup>

<sup>1</sup>Department of Medicinal Chemistry, School of Pharmacy, Lorestan University of Medical Sciences, Khorramabad, Iran.

<sup>2</sup>Department of Biochemistry, School of Medicine, Lorestan University of Medical Science, Khorramabad, Iran.

### Abstract

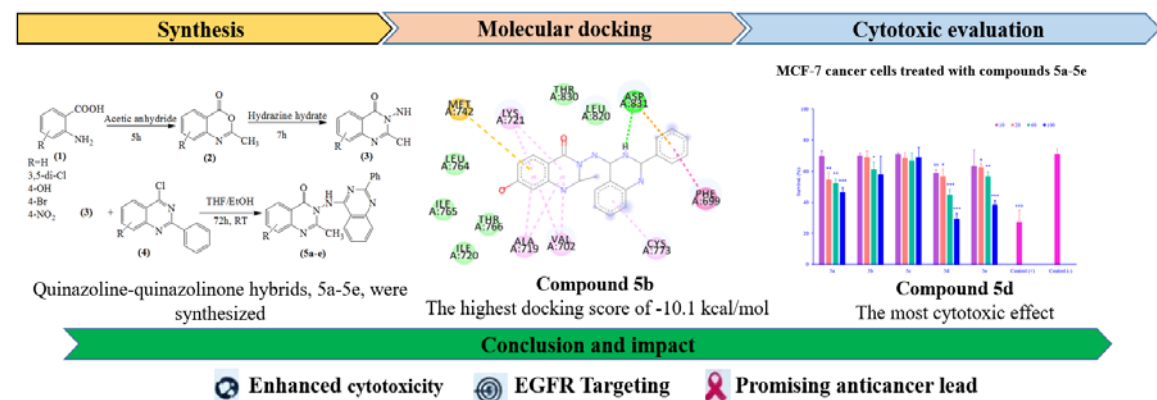
**Background and purpose:** Cancer represents a significant public health challenge and a leading cause of mortality globally. Quinazolinones represent a class of privileged structures that exhibit a broad spectrum of biological activities such as anticancer, antihypertensive, antifungal, antibacterial, and anti-inflammatory properties. In the present study, the synthesis of quinazoline-quinazolinone hybrids as anticancer agents and their cytotoxic evaluation are reported.

**Experimental approach:** Initial studies were done by molecular docking of five analogs of quinazoline-quinazolinone hybrids, erlotinib, and doxorubicin against the epidermal growth factor receptor. Treatment of 3-amino quinazolinone with 4-chloro-2-phenylquinazoline afforded final compounds by the nucleophilic substitution of the chloride with the amine of 3-amino quinazolinone derivatives. The cytotoxic effects of the final compounds were determined *in vitro* against the MCF-7 cell line using the MTT assay.

**Findings/Results:** Compound **5b** (7-hydroxy-2-methyl-3-(2-phenylquinazolin-4-ylamino) quinazolin-4(3H)-one) showed the highest docking score of -10.1 kcal/mol. Additionally, compound **5d** (2-methyl-7-nitro-3-(2-phenylquinazolin-4-ylamino) quinazolin-4(3H)-one) exhibited remarkable *in-vitro* cytotoxic activity at 100  $\mu$ M against the MCF-7 cells.

**Conclusion and implications:** In the present study, quinazoline-quinazolinone hybrids were synthesized, and their cytotoxic effects on the MCF-7 cell line were evaluated. Among them, compound **5d** exhibited the most significant cytotoxic activity. The insertion of a nitro group at the 7 position of quinazolinone enhanced the cytotoxic efficacy against MCF-7 cells, likely attributable to electronic influences. Consequently, this compound could serve as a lead compound in the search for new classes of effective anticancer agents.

**Keywords:** Cytotoxic activity; Hybrid; Molecular docking; Quinazoline; Quinazolinone; Synthesis.



\*Corresponding author: R. Rezaeinasab  
 Tel: +98-6633120243, Fax: +98-6633311944  
 Email: rezaeinasab.rezvan@lums.ac.ir

Access this article online



Website: <http://rps.mui.ac.ir>

DOI: 10.4103/RPS.RPS\_150\_24

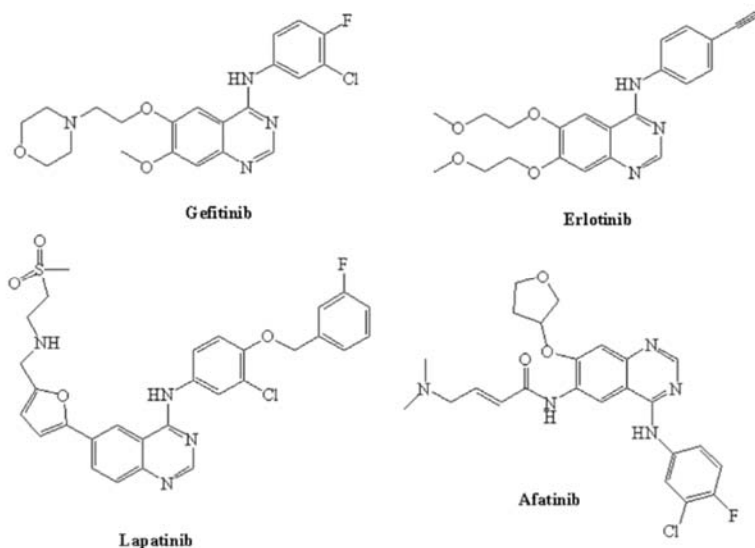


**Fig. 1.** Chemical structures of epidermal growth factor receptor tyrosine kinase inhibitors.

## INTRODUCTION

Cancer is one of the main health complications and the second leading cause of death after cardiovascular diseases in the world (1). Quinazoline derivatives are biologically active molecules that have drawn much attention in pharmaceutical chemistry due to their diverse biological effects, including anticancer, antifungal, antihypertensive, antibacterial, and anti-inflammatory properties (2-4). Quinazoline-based compounds, such as lapatinib, afatinib, erlotinib, and gefitinib, exhibit their anticancer effects primarily via the suppression of the epidermal growth factor receptor (EGFR; Fig. 1) (5). EGFR is a transmembrane protein that plays an important role in normal cellular processes such as cell growth, migration, differentiation, and tumorigenesis (6). Notably, the overexpression of this receptor has been observed in many cancers, including ovarian, breast, colon, and lung cancers (7). Consequently, EGFR is considered a promising target for the design of anticancer agents. Molecular docking is employed to predict the binding free energies between small-molecule ligands and their target receptors (8). Furthermore, the molecular hybridization approach is a well-established synthetic strategy that combines two or more pharmacophore moieties into a single structure to improve potency and minimize side effects (9). Recently, researchers reported quinazoline hybrids as a novel class of anticancer compounds

exhibiting potential EGFR-inhibitory activity (10,11). Based on the pharmacological properties of quinazolinone derivatives, we have incorporated a quinazolinone moiety at the 3 position of a quinazolinone scaffold to create novel hybrid compounds and evaluated their cytotoxic activity. Molecular docking studies targeting EGFR were also performed.

## MATERIALS AND METHODS

All chemicals and solvents utilized in this study were acquired from Merck (Germany) and were used as received, without any additional purification. Infrared (IR, KBr discs) spectra were recorded using a Fourier-transform infrared (FT-IR) spectrophotometer (Nicolet 4700, Thermo Scientific, USA), covering a wavenumber range of 400-4000  $\text{cm}^{-1}$ . The proton and carbon-13 nuclear magnetic resonance ( $^1\text{H}$ NMR and  $^{13}\text{C}$ NMR) spectra were obtained with a Bruker DPX-400 Avance 2 instrument, operating at a frequency of 400 MHz (Germany). The melting points of all synthesized compounds were assessed using an Electrothermal 9300 apparatus (United Kingdom). Thin-layer chromatography (TLC) was employed to monitor the reaction progress and the purity of the synthesized compounds (silica-gel 60 F254, n-heptane: ethyl acetate (EtOAc)). For *in silico* protein-ligand docking simulations, PyRx, Marvin Sketch, Chimera, Open Babel, PyMol, and Discovery Studio Visualizer software packages were used.

The MCF-7 (human breast cancer) cell line was acquired from the Pasteur Institute of Iran (Tehran, Iran). RPMI-1640 culture medium, trypsin-EDTA, and fetal calf serum (FCS) were obtained from Gibco (USA). Dimethyl sulfoxide (DMSO), 3-(4,5-dimethylthiazol-2-yl)-2,5-diphenyltetrazolium bromide (MTT), and doxorubicin were purchased from Merck (Germany). Absorbance measurements were conducted using an ELISA plate reader (Awarwness, USA).

### ***Molecular docking studies***

The chemical structures were drawn using Marvin Sketch software to obtain the SMILES format. All compounds were energy minimized using Chimera software and were subsequently saved in both mol2 and pdb formats. They were then converted into SDF format as a standard file by Open Babel and used in the virtual screening analysis (12). The crystal structure of the EGFR-erlotinib complex was retrieved from the RCSB Protein Data Bank (PDB ID: 1M17) (13). All water and co-crystallized ligands were removed. A grid is established surrounding the active site of EGFR with the coordinates of  $x = 23.535$ ,  $y = 9.845$ ,  $z = 59.393$ . Grid box dimensions were  $93.1 \times 66.5 \times 51.5$  Å, with a  $0.375$  Å grid point spacing for screening. All compounds were docked into the active site of EGFR, and eight docking poses were generated for each compound. The docking procedure was performed using the PyRx screening tool (14).

### ***In-silico physicochemical properties***

The physicochemical properties, including molar refractivity and LogP, were computed utilizing chemical sketchers such as ChemDraw or MarvinSketch software through the two-dimensional structures of the synthesized molecules (15).

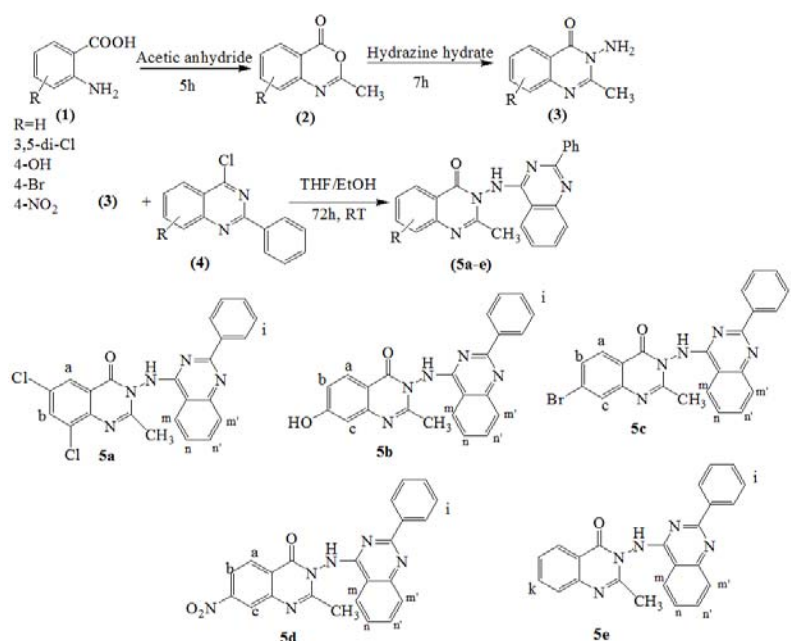
### ***General procedure for the synthesis of compounds 5a-5e***

In a 50 mL two-neck round-bottom flask, a mixture of anthranilic acid (**1**) (1 mmol) with acetic anhydride (10 mL) was refluxed for 5 h to form the benzoxazinone intermediate (**2a-2e**), followed by removal of the excess acetic anhydride under reduced pressure. The reaction between benzoxazinone (1 mmol) and hydrazine hydrate (4 mL) in ethanol (10 mL) under reflux

conditions created 3-amino quinazolinone compounds (**3a-3e**) (16). Treatment of 3-amino quinazolinone (1 mmol) with 4-chloro-2-phenylquinazoline (**4**) (1 mmol) afforded final compounds (**5a-5e**) in tetrahydrofuran (7 mL) and ethanol (3 mL) after 72 h of stirring at room temperature (TLC control). The resulting precipitates were filtered, washed with ethanol, and purified by column chromatography. The slurry method was used to prepare the column. Silica gel (7.5 g) was mixed with the eluting solvent n-heptane (70 mL): EtOAc (30 mL), then poured into a burette (internal diameter of 1 cm). One hundred mg of crude product was loaded onto a silica gel column (16.0 cm in height) and eluted with nine fractions of 3 mL each. Values of  $R_f$  for the components were obtained as 0.51 mm and 0.81 mm for A and B, respectively. To confirm adequate separation, the extracted solution was analyzed by thin-layer chromatography. After removal of the excess of solvent under decreased pressure to afford a white powder (17% yield) (Scheme 1). The structures of synthesized hybrid compounds were confirmed by IR,  $^1\text{H}$ NMR, and  $^{13}\text{C}$ NMR.

### ***Cytotoxic activity***

The cytotoxic activity of all newly synthesized derivatives was assessed using the MTT assay on the MCF-7 cell line (17). The MCF-7 cell line was obtained from the Pasteur Institute of Iran (Tehran, I.R. Iran) and was maintained at a temperature of  $37$  °C in a humidified environment (90%) with 5%  $\text{CO}_2$ . Following 2-3 subcultures,  $180$   $\mu\text{L}$  of cell suspensions ( $5 \times 10^4$  cells/mL) were introduced into 96-well plates and allowed to incubate for 24 h. Stock solutions of the derivatives (10 mM, 1 mL) were prepared using a minimal content of dimethyl sulfoxide (DMSO) and then diluted with the medium to achieve final concentrations of 10, 20, 60, and 100  $\mu\text{M}$ . Following a 24-h incubation period, 20  $\mu\text{L}$  of the different concentrations of the derivatives were combined, and the microplates were subjected to an additional incubation for 48 h. Doxorubicin was utilized as the positive control. To assess cell viability, 20  $\mu\text{L}$  of MTT solution (5 mg/mL in phosphate buffer solution) was added to each well and incubated for 4 h. Subsequently, 150  $\mu\text{L}$  of DMSO was added to each well to dissolve the formazan crystals.



**Scheme 1.** The general strategy for the synthesis of quinazoline-quinazolinone hybrids (**5a-e**).

The absorbance for each well was subsequently assessed at a wavelength of 540 nm utilizing an ELISA plate reader (18,19). Cell viability was determined using the following equation:

$$\text{Cell survival (\%)} = \frac{\text{OD of treated wells} - \text{OD of blank}}{\text{OD of control wells} - \text{OD of blank}} \times 100$$

where OD stands for optical density.

### Statistical analysis

The data are presented as mean  $\pm$  SD,  $n = 3$ . One-way analysis of variance (ANOVA) followed by a Tukey post hoc test was utilized to compare the means.  $P$ -values  $< 0.05$  were considered statistically significant.

## RESULTS

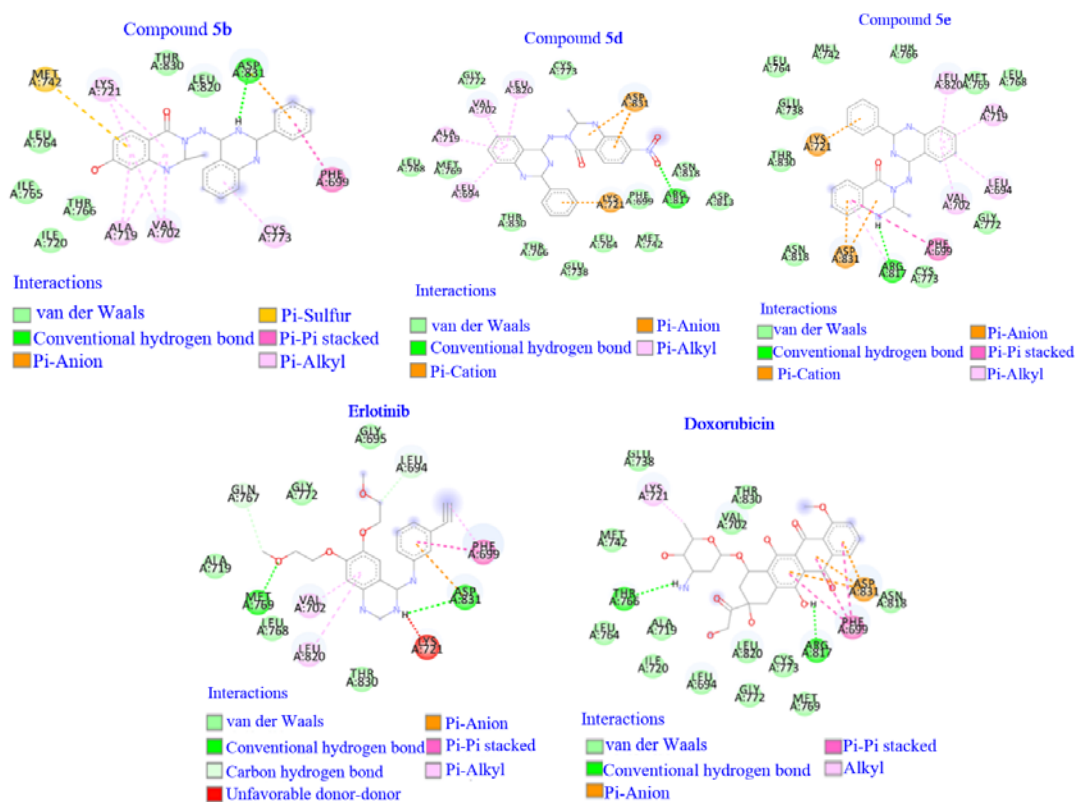
### Molecular docking studies

Upon molecular docking of the designed hybrid compounds within the active site of the EGFR complex structure, most exhibited higher binding affinity than erlotinib (-7.0 kcal/mol) as the reference ligand and doxorubicin (-8.5 kcal/mol) as the standard compound. Table 1 summarizes the binding affinity scores of each synthesized compound, and the docking conformation is exhibited in Figs. 2 and 3. Compound **5b** with the hydroxy

group at the 7 position of the quinazolinone ring seems to be a good lead molecule, which revealed a binding energy of -10.1 kcal/mol. In the case of another compound, **5d**, with a nitro substituent at the 7-position of the quinazolinone ring, it demonstrates a binding energy of -10.0 kcal/mol. As illustrated in Table 1, Figs. 2 and 3, compounds **5b** and **5d** have the potential to form hydrogen bonds with Lys721, Asp831, and Arg817, which may enhance their inhibitory effects. Also, compounds **5b** and **5e**, erlotinib, and doxorubicin exhibited  $\pi$ - $\pi$  interactions with Phe699 as illustrated in Fig. 2. Furthermore, compounds **5d** and **5e**, erlotinib, and doxorubicin demonstrated  $\pi$ -anion interactions with Asp831 (Fig. 2). Compounds **5d** and **5e** also engaged in  $\pi$ -cation interactions with Lys721 (Fig. 2). Moreover, compounds **5b**, **5d** and **5e**, erlotinib, and doxorubicin formed  $\pi$ -alkyl interactions with Lys721, Ala719, Val702, Cys773, Leu694, Leu820, and Phe699 (Table 1 and Fig. 2). Additionally, these compounds effectively stabilized the EGFR by hydrophobic interactions with key residues, including Glu738, Leu694, Leu764, Gly695, Phe699, Ala719, ASN818, Cys773, Val702, Asn818, Gly772, Thr830, Leu820, Ile765, Thr766, Ile720, Leu768, Met769, Thr766, Leu764, Met742, Asp813, Gln767 which are important in hydrophobic contacts (Table 1, Figs. 2 and 3).

**Table 1.** Predicted free energy of binding ( $\Delta G_b$ ), hydrogen bonds, and hydrophobic bonds for new quinazoline-quinazolinone hybrids, erlotinib, and doxorubicin docked into EGFR.

Compound	$\Delta G_b$ (kcal/mol)	Hydrogen bond	Hydrophobic bond	$\pi$ -Alkyl
Lig5a	-9.9	-	Asp831, Lys721, Glu738, Leu764, Asn818, Val702, Leu694, Cys773, Gly833, Gly772, Pro770	-
Lig5b	-10.1	Lys721(2.7Å), Asp831(2.8Å), Asp831(2.3Å)	Ile720, Leu764, Ile765, Thr766, Leu820, Thr830	Lys721, Ala719, Val702, Cys773
Lig5c	-9.9	-	Lys721, Glu738, Met769, Asn818, Phe771, Phe832, Val702, Ala719, Leu764, Cys773, Arg817, Leu834	-
Lig5d	-10.0	Arg817(2.2Å)	Leu768, Gly772, Cys773, Met769, Thr830, Leu764, Thr766, Met742, Phe699, Glu738, Asp813, Asn818	Leu820, Val702, Ala719, Leu694
Lig5e	-9.7	Arg817	THR830, Thr766, Met742, Asn818, Glu738, Met769, Cys773, Gly772, Leu764, Leu768	Leu820, Ala719, Leu694, Val702
Erlotinib	-7.0	Asp831(2.8Å), Met769(1.8Å)	Gly772, Gln767, Leu768, Thr830, Leu694, Gly695, Ala719	Phe699, Leu820, Val702
Doxorubicin	-8.5	Arg817(3.5Å), Cys773(1.9Å), Thr766(2.4Å)	Glu738, Met742, Ile720, Leu820, Thr830, Gly772, Met769, Leu694, Val702, Leu764, Asn818, Ala719	Lys721


**Fig. 2.** Schematic 2D interaction resulting from Discovery Studio visualizer software for compounds **5b**, **5d**, and **5e**, erlotinib, and doxorubicin after molecular docking simulations.

### *In-silico physicochemical properties*

The predicted molar refractivity and LogP

LogP values of the synthesized compounds are given in Tables 2 and 3.

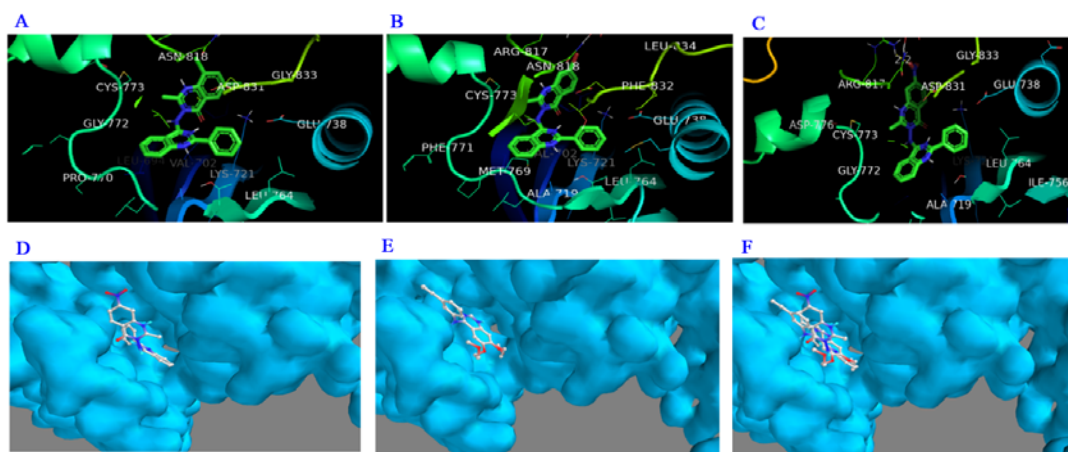


**Fig. 3.** Schematic 3D interaction resulting from PyMol and PyRx software for compounds **5a**, **5c**, **5d**, erlotinib, and superimposed docked image of erlotinib and compound **5d** after molecular docking simulations are shown at images A-F, respectively.

**Table 2.** LogP value of synthesized compounds and doxorubicin.

Compound	LogP value
Lig5a	6.20
Lig5b	4.79
Lig5c	5.84
Lig5d	3.91
Lig5e	5.07
Doxorubicin	1.3

**Table 3.** CMR value of synthesized compounds and doxorubicin.

Compound	CMR value
Lig5a	12.27
Lig5b	11.44
Lig5c	12.06
Lig5d	11.89
Lig5e	11.28
Doxorubicin	13.32

CMR, Calculated molar refractivity.

### Synthesis

#### **6,8-dichloro-2-methyl-3-(2-phenylquinazolin-4-ylamino) quinazolin-4(3H)-one (5a)**

White crystals, yield: 17%, melting point (mp): 280–281 °C, IR  $\nu_{\max}$ , 3440 (NH, str), 3104 (C-H arom, str.), 2999 (C-H aliph, str), 1620 (C=O quinazolinone), 620 (C-Cl)  $\text{cm}^{-1}$ .

$^1\text{H}$ NMR: (400 MHz; DMSO- $d_6$ ):  $\delta$  8.61 (1H, NH, s), 8.50 (1H, s,  $\text{CH}_a\text{-Qu}$ ), 8.48 (1H, s,  $\text{CH}_b\text{-Qu}$ ), 8.30–8.08 (5H, m,  $\text{CH}_i$ ), 7.62–7.56 (2H, m,  $\text{CH}_{m,m'}$ ), 7.54–7.50 (2H, m,  $\text{CH}_{n,n'}$ ), 1.7 (3H, s,  $\text{CH}_3$ ).

#### **7-hydroxy-2-methyl-3-(2-phenylquinazolin-4-ylamino) quinazolin-4(3H)-one (5b)**

Yellowish-white crystals, yield: 15%, mp: 285–286 °C, IR  $\nu_{\max}$ , 3559 (OH, str), 3379 (NH, str), 3236 (C-H arom, str.), 2920 (C-H aliph, str), 1623 (C=O quinazolinone)  $\text{cm}^{-1}$ .

$^1\text{H}$ NMR: (400 MHz; DMSO- $d_6$ ):  $\delta$  8.71 (s, OH), 8.58 (1H, s,  $\text{CH}_c\text{-Qu}$ ), 8.42 (1H, s, NH), 8.17–8.15 (1H, d,  $J=8$  Hz,  $\text{CH}_a\text{-Qu}$ ), 7.88–7.80 (1H, m,  $\text{CH}_b\text{-Qu}$ ), 7.57–7.55 (5H, m,  $\text{CH}_i$ ), 7.32–7.29 (2H, m,  $\text{CH}_{m,m'}$ ), 7.05–6.96 (2H, m,  $\text{CH}_{n,n'}$ ), 1.33 (3H, s,  $\text{CH}_3$ ).

$^{13}\text{C}$ NMR (400 MHz, DMSO- $d_6$ ) in ppm: 161.67 (C=O), 151.81, 149.20, 146.35, 141.70, 140.02, 138.69, 134.99 (aromatic  $\text{C}_{\text{quinazolinone}}$ ), 133.58, 133.16, 132.31, 131.79, 130.71, 129.98, 129.00, 128.76 (aromatic  $\text{C}_{\text{quinazoline}}$ ), 128.47, 128.22, 127.96, 127.35, 126.98, 126.15 (aromatic  $\text{C}_{\text{ph}}$ ), 21.52 ( $\text{CH}_3$ ).

#### **7-bromo-2-methyl-3-(2-phenylquinazolin-4-ylamino) quinazolin-4(3H)-one (5c)**

White crystals, yield: 19%, mp: 288–289 °C, IR  $\nu_{\max}$ , 3534 (NH, str), 3101 (C-H arom, str.), 2910 (C-H aliph, str), 16420 (C=O quinazolinone), 685 (C-Br)  $\text{cm}^{-1}$ .

$^1\text{H}$ NMR: (400 MHz; DMSO- $d_6$ ): 8.73 (1H, s, NH), 8.64 (1H, s,  $\text{CH}_c\text{-Qu}$ ), 8.63–8.61 (1H, d,  $J=8$  Hz,  $\text{CH}_a\text{-Qu}$ ), 8.59–8.55 (1H, m,  $\text{CH}_b\text{-Qu}$ ), 7.53–7.50 (5H, m,  $\text{CH}_i$ ), 7.46–7.40 (2H, m,  $\text{CH}_{m,m'}$ ), 7.36–7.31 (2H, m,  $\text{CH}_{n,n'}$ ), 2.19 (3H, s,  $\text{CH}_3$ ).

$^{13}\text{C}$ NMR (400 MHz, DMSO- $d_6$ ) in ppm: 160.71 (C=O), 145.25, 139.70, 134.03, 133.50, 133.16, 132.20, 131.80 (aromatic  $\text{C}_{\text{quinazolinone}}$ ), 130.71, 130.40, 129.02, 128.76, 128.43, 128.20, 127.95, 127.61 (aromatic  $\text{C}_{\text{quinazoline}}$ ), 127.02, 126.31, 126.10, 121.43, 114.92, 113.21 (aromatic  $\text{C}_{\text{ph}}$ ), 55.74 ( $\text{CH}_3$ ).

**2-methyl-7-nitro-3-(2-phenylquinazolin-4-ylamino) quinazolin-4(3H)-one (5d)**

White crystals, yield: 17%, mp: 280-281 °C, IR  $\nu_{\max}$ , 3300 (NH, str), 3010 (C-H arom, str.), 2840 (C-H aliph, str), 1624 (C=O<sub>quinazolinone</sub>), 1550 (NO<sub>2</sub>), 1450 (NO<sub>2</sub>)  $\text{cm}^{-1}$ .

<sup>1</sup>HNMR: (400 MHz; DMSO-d<sub>6</sub>):  $\delta$  8.71(1H, s, NH), 8.68 (1H, s, CH<sub>c-Qu</sub>), 8.55-8.51 (1H, d,  $J = 16$  Hz, CH<sub>a-Qu</sub>), 8.46-8.42 (1H, m, CH<sub>b-Qu</sub>), 8.20-8.10 (5H, m, CH<sub>i</sub>), 7.98-7.83 (2H, m, CH<sub>m,m'</sub>), 7.79-7.63 (2H, m, CH<sub>n,n'</sub>), 2.30 (3H, s, CH<sub>3</sub>).

<sup>13</sup>CNMR (400 MHz, DMSO-d<sub>6</sub>) in ppm: 161.60 (C=O), 151.80, 149.21, 146.33, 141.76, 140.01, 138.64, 135.01 (aromatic C<sub>quinazolinone</sub>), 133.59, 133.16, 132.11, 131.75, 130.70, 129.97, 129.01, 128.65 (aromatic C<sub>quinazoline</sub>), 128.40, 128.25, 127.90, 127.31, 126.94, 126.11 (aromatic C<sub>ph</sub>), 23.54 (CH<sub>3</sub>).

**2-methyl-3-(2-phenylquinazolin-4-ylamino) quinazolin-4(3H)-one (5e)**

Yellowish-white crystals, yield: 15%, mp: 270-271 °C, IR  $\nu_{\max}$ , 3417 (NH, str), 3344 (C-H arom, str.), 2920 (C-H aliph, str), 1621 (C=O<sub>quinazolinone</sub>) $\text{cm}^{-1}$ .

<sup>1</sup>HNMR: (400 MHz; DMSO-d<sub>6</sub>):  $\delta$  8.54 (1H, s, NH), 8.0-7.82 (4H, m, CH<sub>k</sub>), 7.65-7.60

(2H, m, CH<sub>m,m'</sub>), 7.58-7.53 (2H, m, CH<sub>n,n'</sub>), 7.51-7.47 (5H, m, CH<sub>i</sub>), 1.5 (3H, s, CH<sub>3</sub>).

**Cytotoxic activity**

The cytotoxic effects of derivatives were assessed against the MCF-7 cell line at various concentrations (10, 20, 60, and 100  $\mu\text{M}$ ) using the MTT technique. Results are illustrated in Fig. 4. Compound **5d** demonstrated a significant cytotoxic effect at all tested concentrations on the MCF-7 cell line, with cell viability decreasing to approximately 29% at 100  $\mu\text{M}$  concentration. In contrast, compound **5e** exhibited only mild effects at the same concentrations, resulting in a cell viability reduction to about 38% at 100  $\mu\text{M}$ . Additionally, compound **5a** reduced cell viability to around 46% at 100  $\mu\text{M}$  in contrast to the negative control. Significant differences were not detected among the cytotoxicity of derivatives **5b** (except for 60  $\mu\text{M}$ ) and **5c** on the MCF-7 cell line. These derivatives presented the lowest cytotoxic properties against MCF-7 cells. For these compounds, cell viability decreased to approximately 58% at 100  $\mu\text{M}$  for **5b** and 66% at 60  $\mu\text{M}$  for **5c** ( $\text{IC}_{50} > 100$  for both of them).

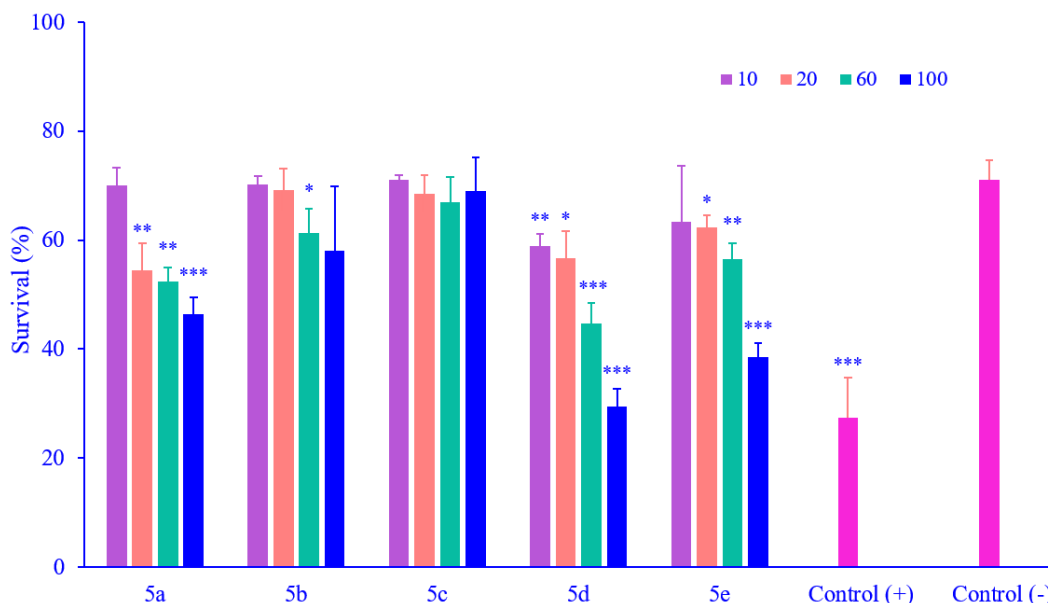


**Fig. 4.** Cytotoxic effect of compounds **5a-5e** on MCF-7 cells following exposure to different concentrations (10, 20, 60, and 100  $\mu\text{M}$ ). Data are presented as mean  $\pm$  SD,  $n = 3$ . \* $P < 0.05$ , \*\* $P < 0.01$ , and \*\*\* $P < 0.001$  indicate significant differences in comparison with the negative control group (untreated cells); doxorubicin was used as the positive control.

## DISCUSSION

Quinazolinone represents a heterocyclic scaffold with a wide spectrum of biological properties, specifically, anticancer activity. Substituted derivatives of quinazolinone at the 2 and 4 positions have been reported as potential anticancer agents (20-22). Quinazolinone is a distinctive template that can be linked to various heterocycles to enhance their effectiveness (23). Benzofuran-appended 4-aminoquinazoline hybrids (5), triazole-substituted quinazoline hybrids (6), and 4-[(2-nitroimidazole-1H-alkyloxy)aniline]-quinazolines (7) are derivatives that exert their anticancer effects through the inhibition of EGFR.

We described the synthesis of a new category of quinazolin-4(3H)-one derivatives, which incorporate a quinazoline moiety at the 3 position of the quinazolinone scaffold in a multi-step reaction process. Initially, a mixture of anthranilic acid and acetic anhydride was refluxed to form a benzoxazinone intermediate (24). Subsequently, the reaction of this intermediate with hydrazine hydrate in ethanol under reflux conditions formed 3-aminoquinazolinone derivatives (25). Finally, treatment of 3-aminoquinazolinone with 4-chloro-2-phenylquinazoline afforded final compounds by the nucleophilic substitution of the chloride with the amine of 3-aminoquinazolinone derivatives (Scheme 1).

Despite all five synthesized compounds exhibiting modest cytotoxic effects, there was an observable trend of growth inhibition that increased with higher concentrations. It seems that the lipophilicity of the compound contributes to challenges in penetrating the membrane. A greater lipophilicity in a compound results in reduced cytotoxic activity owing to restricted membrane partitioning. This limited partition coefficient hinders the ability of these compounds to pass the cell membrane of the MCF7 cell line.

It is suggested that a compound's lipophilicity alone does not adequately reflect its cytotoxic activity, but rather depends more on a balance between hydrophobic and hydrophilic properties (26). The same viewpoint was also expressed, indicating that

compounds with low lipophilicity exhibited greater cytotoxic activity.

The partition coefficient, or log P value, reflects a compound's lipophilicity, with higher values signifying increased lipophilicity of the compound. Table 2 presents a summary of the log P values for all synthesized compounds derived from MarvinSketch predictions, along with the log P values for the reference compound doxorubicin as reported by PubChem. Doxorubicin, a chemotherapy drug, is used to treat cancers like breast cancer. It operates partly by disrupting the activity of DNA (27).

The synthesized compounds exhibited a greater lipophilicity than the standard compound. Doxorubicin may display cytotoxic effects with a log P value of 1.3, whereas the synthesized compounds **5a-e** demonstrated elevated log P values from 3.91 to 6.20. This could influence the uptake of substances on the MCF-7 cell membrane before showing inhibitory effects.

The inhibition of compound **5d** on the MCF-7 cells exhibited a better IC<sub>50</sub> value when compared to the other compounds. This compound, substituted with an electron-withdrawing group (NO<sub>2</sub>), can improve lipophilicity and hydrogen bonding to the receptor, allowing it to pass through the membrane (28).

The shape and size of the synthesized compounds also influence their engagement with the binding site. A large substituent faces obstruction in its interaction with the binding site. Conversely, it can also help the ligand to adjust its orientation for optimal binding interaction.

Polarization and the volume of a compound are measured by molar refractivity. Table 3 presents the ChemDraw Ultra prediction for calculated molar refractivity, indicating that doxorubicin was bigger than the synthesized compound. The synthesized compounds' smaller profile might be a factor influencing the cytotoxic effect associated with binding site interactions (29).

Structure-anticancer activity relationship (SAR) showed that the introduction of substitutions on the phenyl ring influenced the properties of the structures, and the position of

these substitutions also affected the biological activity (30,31). For instance, compound **5d**, which bears an electron-withdrawing substituent (NO<sub>2</sub>) at position 7 of quinazolinone, exhibited enhanced anticancer property against the MCF-7 cell line, likely contributing to its notable effectiveness.

The interaction between the synthesized compounds and the kinase domain of the EGFR protein was assessed. The dock scores of the tested compounds ranged between -9.7 and -10.1 kcal/mol. Compound **5b** revealed the highest dock score of -10.1 kcal/mol and presented a hydrogen bond interaction with Lys721 and Asp831 (Table 1, Figs. 2 and 3). Subsequently, compound **5d** showed the second-highest docking score with the binding energy of -10.0 kcal/mol. These results reflect the good electronegativity and electropositivity profile of the nitro and hydroxyl substituents, which strengthen bonds to the receptor. Protein ligand interactions along with binding energies of quinazoline-quinazolinone derivatives with EGFR are shown in Table 1, Figs. 2 and 3.

In our previous study, we also described the synthesis of a series of quinazoline derivatives as cytotoxic agents against the MCF-7 cell line (24,32). In summary, novel quinazoline-quinazolinone hybrids show promising cytotoxic activities. Compound **5d**, bearing nitro, showed the highest inhibitory activity against the proliferation of the MCF-7 cell line. The docking results were in parallel correlation with *in vitro* cytotoxic activity.

## CONCLUSION

In the current investigation, quinazoline-quinazolinone hybrids were synthesized and assessed for their cytotoxic effects on the MCF-7 cell line. Among them, compound **5d** (2-methyl-7-nitro-3-(2-phenylquinazolin-4-ylamino) quinazolin-4(3H)-one) showed the most significant cytotoxic activity with reduced cell viability to approximately 29% at 100 μM (IC<sub>50</sub> = 26.92 ± 8.24) against the MCF-7 cell line. Substitution of the nitro group at the 7 position of quinazolinone appears to enhance the cytotoxic properties, likely due to electronic effects. In docking studies, all derivatives were able to interact in a manner close to the known

inhibitors with the residues situated in the EGFR binding site. The highest docking score achieved in this series was -10.1 kcal/mol for compound **5b** (7-hydroxy-2-methyl-3-(2-phenylquinazolin-4-ylamino) quinazolin-4(3H)-one). This research suggests that quinazoline-quinazolinone hybrids may serve as a promising scaffold for the advancement of EGFR inhibitors and could contribute to the discovery of new classes of effective anticancer agents.

## Acknowledgments

This study was approved by the Ethics Committee of Lorestan University of Medical Sciences (code: IR. LUMS. REC. 1400.149. and IR. LUMS. REC 1400.260.)

## Conflict of interest statement

All authors declared no conflict of interest in this study.

## Authors' contributions

R. Rezaeinasab conducted molecular docking, compound synthesis, structure elucidation, and wrote the article; M. Hormozi and S. Rahimi conducted cytotoxic evaluation assay; M. Azarmi contributed to synthesizing the compounds. All authors have read and approved the finalized article. Each author has fulfilled the authorship criteria and affirmed that this article represents honest and original work.

## AI declaration

The authors did not use any AI-assisted technologies in the preparation of this manuscript.

## REFERENCES

- Hawata MA, El-Sayed WA, Nossier ES, Abdel-Rahman AAH. Synthesis and cytotoxic activity of new pyrimido[1,2-c]quinazolines, [1,2,4]triazolo[4,3-c]quinazolines and (quinazolin-4-yl)-1H-pyrazoles hybrids. *Biointerface Res Appl Chem*. 2022;12:5217-5233. DOI: 10.33263/BRIAC124.52175233.
- Keikhosravi N, Dehghan-Ghahfarokhi E, Abdollahi S, Piramoon M, Ghasemian-Yadegari J, Rezaeinasab R. Solvent-free synthesis and antimicrobial activity of dihydroquinazolinone derivatives. *J Med Chem Sci*. 2022;5:308-314. DOI: 10.26655/JMCHEMSCI.2022.3.3.

3. El-Shershaby MH, Bayoumi AH, Ghiaty A, Abulkhair HS. Synthesis and pharmacological evaluation of some new 1,2,4-triazolo quinazoline derivatives. *Az J Pharm Sci.* 2021;64:69-79. DOI: 10.21608/ajps.2021.187755.
4. Alqahtani AS, Ghorab MM, Nasr FA, Ahmed MZ, Al Mishari AA, Attia SM. *et al.* Cytotoxicity of newly synthesized quinazoline-sulfonamide derivatives in human leukemia cell lines and their effect on hematopoiesis in zebrafish embryos. *Int J Mol Sci.* 2022;23:4720,1-17. DOI: 10.3390/ijms23094720.
5. Mphahlele MJ, Maluleka MM, Aro A, McGaw LJ, Choong YS. Benzofuran-appended 4-aminoquinazoline hybrids as epidermal growth factor receptor tyrosine kinase inhibitors: synthesis, biological evaluation and molecular docking studies. *J Enzyme Inhib Med Chem.* 2018;33:1516-1528. DOI: 10.1080/14756366.2018.1510919.
6. Banerji B, Chandrasekhar K, Sreenath K, Roy S, Nag S, Saha KD. Synthesis of triazole-substituted quinazoline hybrids for anticancer activity and a lead compound as the EGFR blocker and ROS inducer agent. *ACS Omega.* 2018;3:16134-16142. DOI: 10.1021/acsomega.8b01960. Epub 2018 Nov 28.
7. Cheng W, Wang S, Yang Z, Tian X, Hu Y. Design, synthesis, and biological study of 4-[(2-nitroimidazole-1H-alkyloxyl)aniline]-quinazolines as EGFR inhibitors exerting cytotoxicities both under normoxia and hypoxia. *Drug Des Devel Ther.* 2019;13:3079-3089. DOI: 10.2147/DDDT.S209481.
8. Seydbagian N, Dehghan-Ghahfarokhi E, Abdollahi S, Rezaeinasab R. Synthesis, antimicrobial activity and molecular docking study of novel N,2-diphenylquinazolin-4-amine derivatives. *Iran J Pharm Sci.* 2023;19(1):1-10. DOI: 10.22037/ijps.v19i1.43111.
9. Wu WY, Cao SL, Mao BB, Liao J, Li ZF, Song HB, *et al.* Synthesis and antiproliferative evaluation of hybrids of indolin-2-one and quinazoline-4(3H)-one linked *via* imine bond. *Lett Drug Des Discov.* 2013;10:61-66. DOI: 10.2174/1570180811309010061.
10. Bathula R, Mondal P, Raparla R, Satla SR. Evaluation of antitumor potential of synthesized novel 2-substituted 4-anilinoquinazolines as quinazoline-pyrrole hybrids in MCF-7 human breast cancer cell line and A-549 human lung adenocarcinoma cell lines. *Futur J Pharm Sci.* 2020;6:1-11. DOI: 10.1186/s43094-020-00059-5.
11. Hassanzadeh F, Sadeghi-aliabadi H, Nikooei S, Jafari E, Vaseghi G. Synthesis and cytotoxic evaluation of some derivatives of triazolequinazolinone hybrids. *Res Pharm Sci.* 2019;14:130-137. DOI: 10.4103/1735-5362.253360.
12. Noser AA, El-Naggar M, Donia T, Abdelmonsef AH. Synthesis, *in silico* and *in vitro* assessment of new quinazolinones as anticancer agents *via* potential AKT Inhibition. *Molecules.* 2020;25:4780. DOI: 10.3390/molecules25204780.
13. Emami L, Sabet R, Khabnadideh S, Faghieh Z, Thayori P. Quinazoline analogues as cytotoxic agents; QSAR, docking, and *in silico* studies. *Res Pharm Sci.* 2021;16(5):528-546. DOI: 10.4103/1735-5362.323919.
14. Zare S, Emami L, Faghieh Z, Zargari F, Faghieh Z, Khabnadideh S. Design, synthesis, computational study and cytotoxic evaluation of some new quinazoline derivatives containing pyrimidine moiety. *Sci Rep.* 2023;13:14461. DOI: 10.1038/s41598-023-41530-6.
15. Naeem S, Akhtar S, Zafar, Iqbal S. *In-silico* determination of pKa and logp values of some isoniazid synthetic analogues using Marvin software. *Pak J Pharm Sci.* 2020;33(2):715-719. DOI: 10.36721/PJPS.2020.33.2.REG.715-719.1.
16. Nasab RR, Mansourian M, Hassanzadeh F. Synthesis, antimicrobial evaluation and docking studies of some novel quinazolinone Schiff base derivatives. *Res Pharm Sci.* 2018;13(3):213-220. DOI: 10.4103/1735-5362.228942.
17. Li W, Chen SY, Hu WN, Zhu M, Liu JM, Fu YH, *et al.* Design, synthesis, and biological evaluation of quinazoline derivatives containing piperazine moieties as antitumor agents. *J Chem Res.* 2020;44:536-542. DOI: 10.1177/1747519820910384.
18. Hassanzadeh F, Sadeghi-Aliabadi H, Jafari E, Sharifzadeh A, Dana N. Synthesis and cytotoxic evaluation of some quinazolinone-5-(4-chlorophenyl) 1, 3, 4-oxadiazole conjugates. *Res Pharm Sci.* 2019;14:408-413. DOI: 10.4103/1735-5362.268201.
19. Wu X, Li M, Tang W, Zheng Y, Lian J, Xu L, *et al.* Design, synthesis, and *in vitro* antitumor activity evaluation of novel 4-pyrrolamino quinazoline derivatives. *Chem Biol Drug Des.* 2011;78:932-940. DOI: 10.1111/j.1747-0285.2011.01234.x.
20. Wang XM, Xin MH, Xu J, Kang BR, Li Y, Lu SM. Synthesis and antitumor activities evaluation of m-(4-morpholinoquinazolin-2-yl)benzamides *in vitro* and *in vivo*. *Eur J Med Chem.* 2015;96:382-395. DOI: 10.1016/j.ejmech.2015.04.037. Epub 2015 Apr 17.
21. Mortazavi M, Eskandari M, Moosavi F, Damghani T, Khoshneviszadeh M, Pirhadi S, *et al.* Novel quinazoline-1,2,3-triazole hybrids with anticancer and MET kinase targeting properties. *Sci Rep.* 2023;13:14685. DOI: 10.1038/s41598-023-41283-2.
22. Sonousi A, Hassan RA, Osman EO, Abdou AM, Emam SH. Design and synthesis of novel quinazolinone-based derivatives as EGFR inhibitors with antitumor activity. *J Enzyme Inhib Med Chem.* 2022; 37:2644-2659. DOI: 10.1080/14756366.2022.2118735.
23. Abu-Hashem AA, Hakami O, Amri N. Synthesis, anticancer activity and molecular docking of new quinolines, quinazolines and 1,2,4-triazoles with pyrido[2,3-d] pyrimidines. *Heliyon.* 2024;10:e26735. DOI: 10.1016/j.heliyon.2024.e26735.

24. Nasab RR, Karami B, Khodabakhshi S. Selective solvent-free Biginelli condensation using tungstate sulfuric acid as powerful and reusable catalyst. *Bull Chem React Eng Catal.* 2014;9:148-154. DOI: 10.9767/brec.9.2.6794.148-154.
25. Rezaeinasab R, Jafari E, Khodarahmi G. Quinazolinone-based hybrids with diverse biological activities: A mini-review. *J Res Med Sci.* 2022;27:68. DOI: 10.4103/jrms.jrms\_1025\_21.
26. Nasab RR, Hassanzadeh F, Khodarahmi GA, Mirzaei M, Rostami M, Jahanian-Najaf Abadi A. Synthesis, characterization, cytotoxic screening, and density functional theory studies of new derivatives of quinazolin-4(3H)-one Schiff bases. *Res Pharm Sci.* 2017;12:444-455. DOI: 10.4103/1735-5362.217425.
27. Masoudinia S, Samadzadeh M, Safavi M, Bijanzadeh HR, Foroumadi A. Novel quinazolines bearing 1,3,4-thiadiazole-aryl urea derivative as anticancer agents: design, synthesis, molecular docking, DFT and bioactivity evaluations. *BMC Chemistry.* 2024;18:30. DOI: 10.1186/s13065-024-01119-0.
28. Perez-Fehrmann M, Kesternich V, Puelles A, Quezada V, Salazar F, Christen P, *et al.* Synthesis, antitumor activity, 3D-QSAR and molecular docking studies of new iodinated 4-(3H)-quinazolinones 3N-substituted. *RSC Adv.* 2022;12:21340. DOI: 10.1039/d2ra03684c.
29. Kciuk M, Gielecińska A, Mujwar S, Kołat D, Kałuzińska-Kołat Z, Celik I, *et al.* Doxorubicin, an agent with multiple mechanisms of anticancer activity. *Cells.* 2023;12:659. DOI: 10.3390/cells12040659.
30. Ahmed MF, Magdy N. Design, synthesis and biological evaluation of some novel substituted quinazoline derivatives as antitumor agents. *Acta Pol Pharm.* 2018;75:669-677. DOI: 10.1016/j.ejmech.2014.04.029.
31. Malhotra A, Bansal R, Halim CE, Yap CT, Sethi G, Kumar AP, *et al.* Novel amide analogues of quinazoline carboxylate display selective anti-proliferative activity and potent EGFR inhibition. *Med Chem Res.* 2020;29:2112-2122. DOI: 10.1007/s00044-020-02634-0.
32. Rafian-boroujeni M, Rezaeinasab R, Bahrami N. One-pot synthesis, cytotoxic evaluation and molecular docking of 3,4,7,8-tetrahydroquinazoline-2,5-(1H,6H)-dione derivatives on EGFR. *Int Pharm Acta.* 2022;5(1):e5. DOI: 10.22037/ipa.v5i1.38025.